# Silicon Nanomembranes as an Enabling Platform for Multifunctional Microsystems

Greg Madejski, University of Rochester, Biomedical Engineering

Advisor
James McGrath, PhD, University of Rochester

Committee Members
Richard Waugh, PhD, University of Rochester
Benjamin Miller, PhD, University of Rochester
Kevin Webb, PhD, University of Nottingham

External Examiner
Lisa DeLouise, PhD, University of Rochester

# Specific Aims

Microsystem technology is invaluable in healthcare as it creates useful information efficiently through the miniaturization of sensors, fluidics, and machinery. However, there are problems miniaturizing microsystem elements that use many different technologies to achieve their function. Electrical leads, sensors, and flow channels rely on different materials, manufacturing flows, and do not scale down with the same behavior, while microfluidic systems suffer from the lack of efficiency introduced by extraneous dead volume. A generalizable microsystem platform that could overcome these challenges would be desirable.

We submit that silicon nanomembrane technology can serve as a miniaturization platform to integrate biomedical devices. The advent of silicon nanomembrane technology [1] has created unique opportunities for localizing filtration [2], shear free microfluidics [3], pumps [4], and mixers (unpublished) to highly scalable chip formats. Our goals in this proposal are to demonstrate the flexibility of the nanomembrane platform to solve problems in the design of biomedical microsystems (Aims 1 and 2) and to demonstrate the ability of the nanomembrane platform to perform multiple functions (Aim 3).

**Aim 1 – Fabrication of Nanomembrane Tented Structures to Extend the Lifetime of Delicate Sensing Devices**

The cost of DNA sequencing has dramatically fallen in the last decade due to the invention of single-biological nanopore devices. Solid state nanopores (ssNPs) promise better shelf-life and even lower costs but are more prone to fouling and failure. The *in situ* integration of silicon nanomembranes within hundreds of nanometers of a ssNP will block potential fouling particulates and extend the lifetime of sequencing. Fabrication strategies will include face-to-face bonding of nanomembrane and ssNP chips as well as direct nanomembrane transfer to ssNP chips. Devices will be tested for the ability to filter particulates in Rochester before DNA-based testing by collaborators in Ottawa, CA.

**Aim 2 – Fabrication of Raman-Silent Nanomembranes to Enable the Chemical Fingerprinting of Cellular Components by Raman Spectroscopy.**

Raman spectroscopy is a powerful technique that can noninvasively identify biomolecular signatures in tissue preparations [5], but is limited when dealing with isolated cells due to relatively larger background signals from the substrate. Materials with low background signals, such as magnesium fluoride ($MgF_2$) are used to overcome this problem, but lack porous structure necessary for the establishment of proper epithelial cell physiology. Using a combination of evaporation and reactive ion etch, we will create a $MgF_2$ nanomembrane using a silicon nitride nanomembrane as a template. Material characterization (pore size via SEM, purity via EDS, mechanical burst pressure strength, biocompatibility via Live/Dead kit) will be performed in Rochester before functional Raman testing occurs with the help of collaborators in Nottingham, UK.

**Aim 3 – Integration of Nanomembrane Operations to Create a Multilmodal Measurement System for the Study of Water Transport through Retinal Epithelial Monolayers**

Isotonic water transport is one of the hallmarks of a properly functioning epithelial cell barrier, the precise nature of which is referred to as 'one of the great unsolved problems' in retinal epithelial physiology [6]. We will create a microsystem that integrates nanomembrane pumps, sensors and scaffolds to build a more comprehensive model of epithelial fluid transport using silicon nanomembrane technology and Raman spectroscopy. Electroosmotic pumping will be used to perfuse the system while streaming potentials measurements will quantify the rate of active water transport by epithelial cells, grown on nanoporous $MgF_2$ substrates. Bulk water transport measurements will be compared to Raman measurements of deuterated water transport across epithelial layers.

## Significance

Biomedical lab-on-a-chip (LOC) technologies involve glass or silicon-based chips with microfluidic channels and chambers, as well as electronics, optics, and plumbing elements [7-9]. These components work together to sample, transport, react, separate and detect small quantities of biological or chemical substances [10-13]. Despite the revolutionary promise of LOC technologies, there are many practical problems that arise when trying to make complex systems. Each LOC miniaturization effort presents a unique set of challenges, driven by material constraints, sensor constraints, and physical size constraints. The dominant PDMS microfluidic technologies have a large body of research detailing ways to fashion pumps and filters and integrate sensors. However, most of these strategies require complicated implementations like pneumatics [14] or phase change metals [15], additional fabrication to make a low yield photolithographic pump [16, 17], or bulky supporting equipment. It is wasteful and awkward to add backend integration of large pumps, sensors, and filters to miniaturized devices, especially when the microsystem application has no inherent need for a macroscopic scale.

Developing and characterizing modules that could be readily integrated into a miniaturization process is one key to accelerating the development of further LOC technologies. The integrated fabrication and placement of miniaturized pumps, sieves, detectors, and supports would be significant because it would reduce dead volumes and overall system footprint while enabling 'bioprocess circuits' to be easily designed on chips (Figure 1). This proposal aims to illustrate that the process flexibility of the nanomembrane platform could enable integrated bioprocessing and sensing chips.

ssNP sensors are cheaper to fabricate and easier to use than biological nanopores [18]. However, the lifetime of the ssNP sensor is currently limited by clogging/fouling of the ssNP surface by agglomerates present in what is already considered a “clean” sample [19]. Biomedical applications will require robust ssNP that detect biomarkers extracted from assays performed in complex biological samples. Nanomembranes integrated at the site of the sensor could efficiently remove irrelevant particles that would permanently damage the sensor.

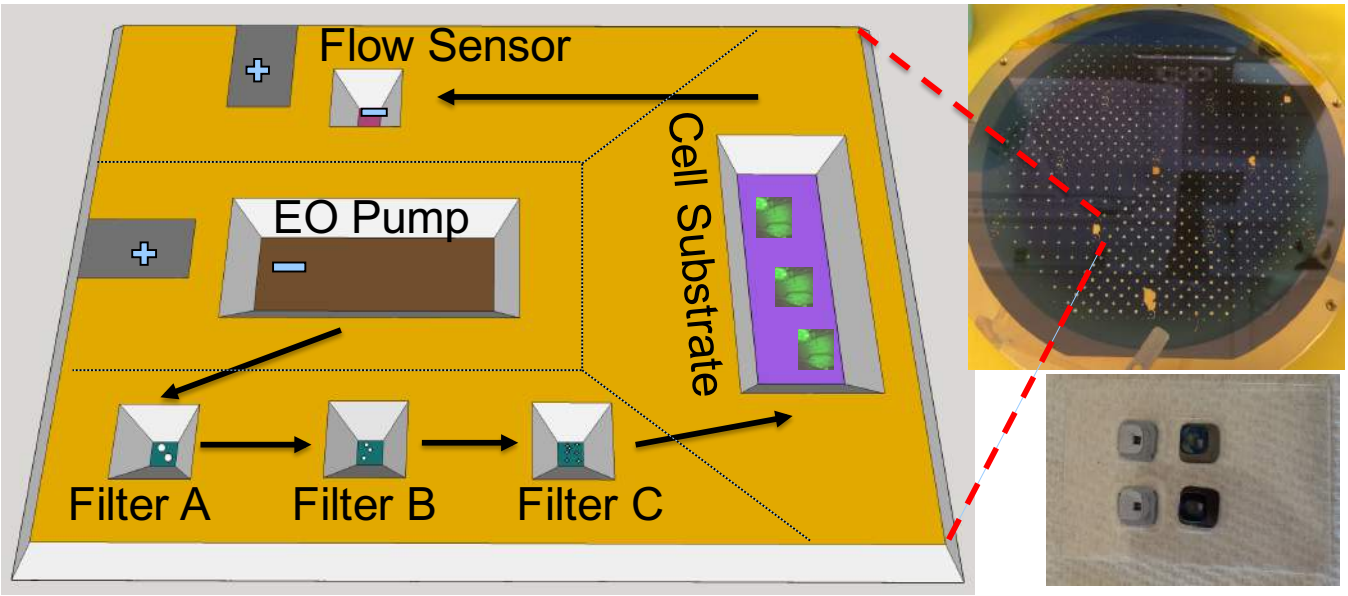


Figure 1 - Nanomembranes as Microsystem Elements. *Left*: Cartoon of a theoretical silicon nanomembrane microsystem used to pump filtered fluid past a cell culture substrate, detecting the flow rate simultaneously. Differently colored membranes have different nanomembrane properties (porosity, materials, pore size). *Top Right*: Hundreds of nanomembrane microsystems can be fabricated at scale using the techniques of the semiconductor industry. *Bottom Right*: In lieu of a custom-designed microsystem, individual nanomembrane elements can be added into other process flows (laminate microfluidics shown, chips are 5.4 mm squares).

Furthermore, nanopore-based biomarker-sensing technologies could have a significant impact beyond DNA sequencing, as a tool used in disease diagnostics in point-of-care applications by screening proteins at very low concentrations from very small sample volumes, profiling microRNA expression, and performing epigenetic and genetic mutation analysis.

The addition of nanomembrane technology to LOC barrier tissue models creates a significant benefit to improving the quality of the model, by promoting the proper formation and polarization of cells through increased permeance of the substrate. Disease processes like macular degeneration originate from the dysregulation of epithelial fluid transport [20, 21]. Understanding the essential biophysics behind this process would offer an avenue for the development and application of targeted therapeutic intervention by manipulating epithelial transport, physiology, and barrier function. The creation of $MgF_2$ nanomembranes enable non-invasive Raman spectroscopy to measure the molecular transport of water and other biomolecules across cultured retinal epithelial barriers. Our system will combine label-free molecular imaging with traditional measures of epithelial physiology such as cell morphology, cell-cell junction integrity, and membrane potential. These tools will result in multidimensional data sets that give unprecedented insight into epithelial physiology.

Overall, silicon nanomembrane system complexity and miniaturization is traded off by the increased complexity and length of the manufacturing process. However, these processes are well understood and will ultimately provide a system that is easier to operate in a small environment. Combining pumping, sensing, sieving, and material choices into a LOC system will allow for miniaturization and integration specific to a particular biological problem using a standard platform, eliminating dead volumes that would normally arise from this process.

## Innovation

The silicon nanomembrane platform simplifes a number of different operations desirable in microsystems, integrating a variety of functions that are not easily performed using current membrane and microsystems technology. Simply used as a filter, silicon nanomembranes have been shown to have excellent size separation characteristics, where 5 nm resolution separations were achieved with gold nanoparticles [2]. DNA nanopore sequencing microsystems can benefit from these nanomembranes by screening out unwanted particulates near the nanopore, improving the lifetime and sensitivity of these devices [22]. At present, electroosmotic-pumping microsystems are often limited by high voltages (> 20 V) and vapor bubbles from electrolysis products, which will eventually clog the microsystem, arresting flow. Recently, porous nancorystalline silicon (pnc-Si) membranes have demonstrated pumping characteristics that are over 25x better than other technologies [4]. The successful deployment of this technology will create practical microsystems that operate in a low-voltage regime (1-10 V) that do not create clogging products, moving microliters of fluid at microliter flow rates (0.1-1 mL/min). Flow detection using streaming potential measurements will benefit from the same miniaturization of nanomembranes. In turn, this will provide microliter-level flow resolution due to the increased voltage generation from flow through the nanopores. Material choices can also be made to improve the sensitivity of optical metrology in a microsystem, which would be useful in a LOC tissue model. Creating thin sheets of porous $MgF_2$ allows for the miniaturization and integration of a LOC tissue model that can use Raman spectroscopy to characterize cells *in vitro*. Systems that incorporate these substrates will impact our understanding of barrier-function diseases in LOC tissue models, by creating more realistic cell environments (permeance effects cell morphology) without interfering with measurement. Overall, it is innovative to tackle the problems of miniaturization using nanomembrane elements to perform the essential activities of a microsystem.

# Specific Aim 1 Approach

## Hypothesis and Rationale

DNA sequencers will be an important part of personalized medicine. “Big Data” systems that use personalized sequencing information have already entered the market to inform treatment plans for cancerous diseases [23]. At present, the cost of reading a DNA sequence needs to fall in order to increase the utilization and effectiveness of these systems. One way to improve the value of devices is to increase their effective lifetime. Recently, there have been many successful attempts to bring down the cost of nanopore sequencers, some with biological nanopores [24, 25], and recently with solid state silicon nanopores [26, 27]. Biological nanopores have been the dominant choice of commercial interests [27, 28], but ssNPs can be made cheaply and incredibly sensitive to purified samples such that they can detect a single DNA base pair passing through [29]. However, failure in the sensitive ssNP can occur due to non-specific clogging caused by stiction, resulting in erroneous current measurements [19]. It would be desirable to reduce the ability of potential clogging products to impact the functioning of these devices at the site of the nanopore, but without impacting the strength of the technique.

We hypothesize that an ultrathin nanomembrane can be integrated above a ssNP to filter out non-specific particulates and larger DNA configurations in the system, while not compromising the system’s ability to electrically sense the passage of DNA. Silicon nanomembranes are ideal for improving this system because of their low hydraulic and electrical resistance, while maintaining the ability to perform separations. The close integration of the nanomembrane with the sensor is necessary to prevent interference with the DNA capture radius of the ssNP (sub micron), while still allowing larger DNA fragments to be threaded into the ssNP. The multitude of pores in the nanomembrane filter suspended above the ssNP allow for continuing filtration even after individual pores are closed. The successful completion of this Aim will have demonstrated the addition of silicon nanomembrane technology into microsystems as localized upstream filters, improving the lifetimes of sensitive detectors.

## Research Design

### 1.1 Integration of Silicon Nitride Nanomembranes and Target Chips at sub-Micron Distances

The goal of this study is to position a nanomembrane 100 nm upstream of a target ssNP membrane to serve as a prefilter. This is not trivial due to two potential problems: i) fabrication of the structure without compromising the sensor material below and ii) wetting the space in between the nanomembrane and sensor substrate. The latter concern has been challenging in previous separation experiments given the ability of nanoporous membranes to maintain air/water interfaces against any practical transmembrane pressure [2]; membrane rupture will occur before forcing water through the nanomembrane. As for the first problem, it is known that wafers can be joined using anodic bonding [30], so we created a setup to join two silicon chips together at 500 C and 700 V. Nanomembrane transfers were successful, but the supporting transfer chips broke off, meaning that the weld was unsuccessful on a large scale. Examination by scanning electron microscopy (SEM) revealed large capillary networks formed around the posts by nanomembranes giving the appearance of wrinkles. Further experimentation was performed by manually ripping off membranes and forcing them onto a substrate chip. This method of transfer was unreliable, until a stray observation was made: wet breath exhalations near the chip smoothed out and dropped sheets of nanomembrane onto the

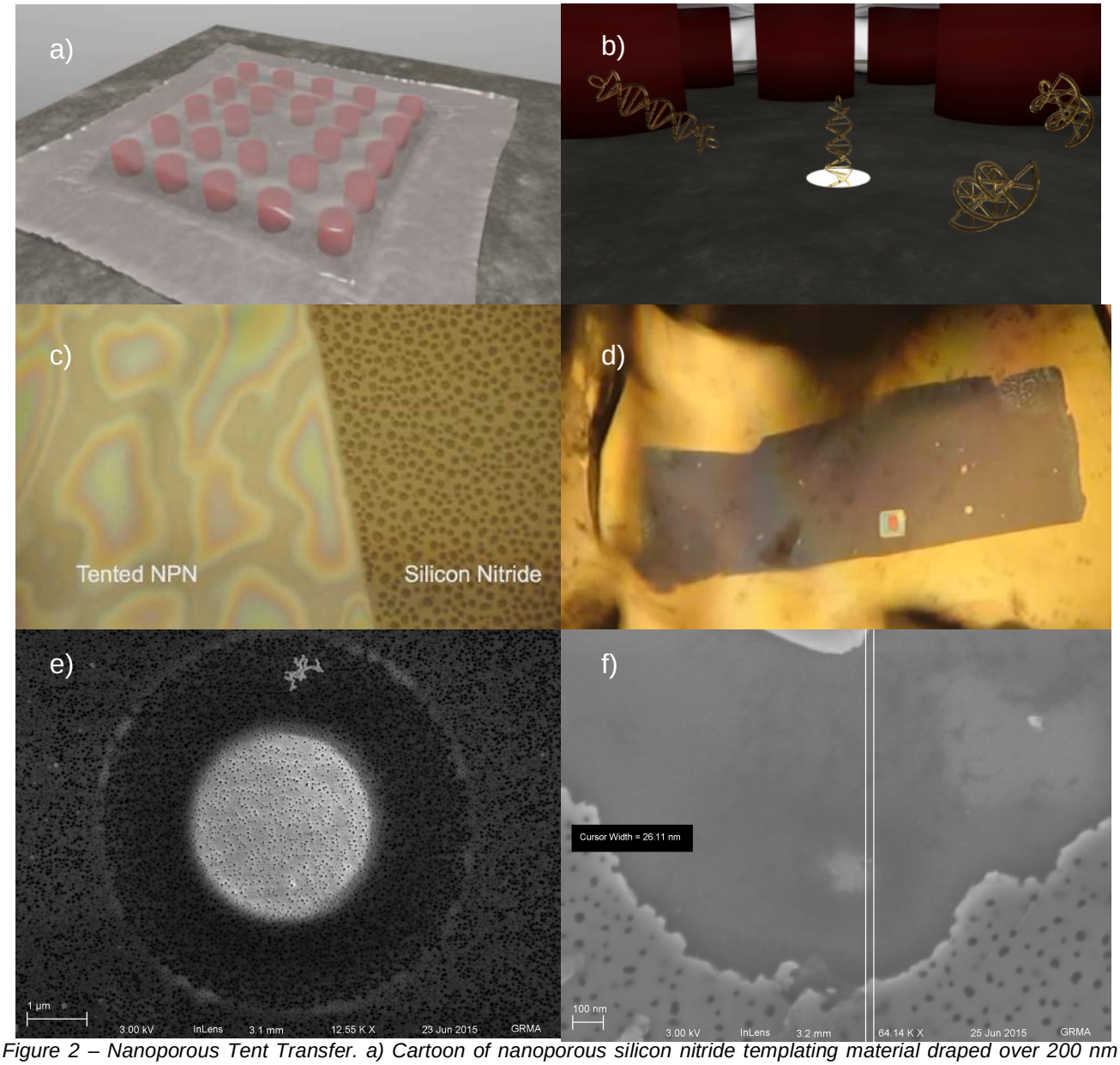


*Figure 2 – Nanoporous Tent Transfer. a) Cartoon of nanoporous silicon nitride templating material draped over 200 nm tall oxide pillars b) DNA will migrate through the tent and enter the nanopore sequencer below. c) Tented material has different wetting behavior (Newton's colors) than the substrate surface d) 2 mm x 0.7 mm tented nanomembrane is stable under 3 dynes/cm$^2$ of shear stress on silicon nitride. e) SEM image displays filtration properties of the tent, screening a 60 nm Au nanoparticle aggregate from the suspended surface (dark annulus). f) Broken tent shows 20 nm nanoparticles on the inner substrate surface.*

surface. If there is water in between the nanomembrane and the sensor substrate, problem ii) is not a concern because water from the transfer is already hydrating the space, as well as empirically solving problem i) by providing a local delamination mechanism.

We now propose to use a novel method to transfer membranes onto a hydrophobic surface to create a 'tented' structure. The substrate chip will contain small repeating post features, 1-3 µm in diameter, with a height of 200 nm, providing the necessary structural perturbation to drape a 50 nm thick nanoporous silicon nitride (NPN) nanomembrane over the surface, forming small cavities (~0.5 fL) around the features (Figure 2a). We will clamp a sacrificial membrane chip to a target substrate chip and delaminate the NPN membrane using boiling water vapor, where the membrane is fixed to the substrate chip by the thin water vapor layer. We will test the stability of the structures by flowing particulate tangential to the surface,

shearing the nanomembrane and examining the position of the nanomembrane under a brightfield microscope.

Based on the hypothesis that thin layers of water are providing the necessary adhesion to the substrate, we will develop a model using van der Waal's forces, capillary action, and the mass properties of the nanomembrane to determine if there are critical levels for disrupting the nanomembrane with shear in a microsystem. We will use silicon nitride nanomembranes with a range of thicknesses (20, 40, 120 nm) and pore sizes (35 nm, 3 μm) to observe if there are differences in the contact strength of the tenting layer, and a nonporous nanofilm (20 nm) as a control surface, as water is sheared over the surface (Figure 2d). We will also test the stability of the bond between different types of substrates (silicon nitride, glass, plastic). Similarly, differential interference contrast (DIC) imaging will be used to capture the colors of the film in order to quantify how thick the water layer is underneath the nanomembrane (Figure 2c)

### 1.2 Demonstration of Filtration Upstream of Target Substrates

To test the ability of a nanoporous tent to serve as a filter, we will incubate a tented structure with 20 nm and 60 nm gold particulates for a period of 2 hours. We anticipate that the larger gold particulates will not pass through the tented structure (given an average pore size of 30 nm) into the attocavity below (Figure 2e). Using SEM, we will observe the surface of the tented structure, then fracture the tent and observe the size of particulates that migrate into the attocavity space (Figure 2f). This work will confirm that the tent can provide size discrimination required to separate out a DNA clump (50 nm) that would clog a nanopore sequencer.

### 1.3 Measurement of ssNP Lifetime with Integrated Nanomembrane Prefilters

A DNA nanopore sequencer chip will be fabricated using a substrate chip (20 nm thin silicon nitride nanomembrane with a 200 nm oxide spacer structure) and a sacrificial nanomembrane tenting chip (NPN, average pore size = ~30 nm, porosity = 15-20%) using the fabrication process described in Section 1.1. Devices fabricated in Rochester will be tested by the Tabard-Cossa laboratory at the University of Ottawa. The chip will then be clamped into a pore drilling device, and the sensing pore will be drilled using a dielectric breakdown method with a nanoporous tent in place (Appendix I) [18]. DNA translocation events will be observed by introducing a range of base pair lengths (5 bp – 5000 bp) and evaluating the current from one side of the nanopore to the other (Figure 2b). The tented structures should last longer before clogging on average compared to sequencer chips without the extra filtration from the same DNA solution.

## Expected Outcomes

The successful completion of this Aim will produce low-cost DNA sequencing chips that have improved lifetimes through the addition of a silicon nanomembrane filter. Nanomembrane tent structures will have been characterized for insertion into other microsystems. The material and fabrication technology inherent to the silicon nanomembrane platform is useful for integration into other microsystems that need additional simple nanofiltration.

## Potential Problems and Alternative Solutions

Although the nanomembrane tent has been placed down in practice, it is not chemically bonded to the substrate underneath. Therefore, it is possible for materials to migrate around and underneath the tented area rather than through the nanomembrane. Considering the relatively high permeability of the combined nanopores in parallel, the relative probability of the

migration around the tent should be much less than through the tent. If the migration around the tent becomes a problem, it would be possible to weld the tenting chip on top of the substrate chip using anodic bonding or PDMS, but these methods add an additional layer of complexity and may negatively impact device performance.

# Specific Aim 2 Approach

## Hypothesis and Rationale

Silicon nanomembrane technology is very adaptable, however, silicon is not necessarily the optimal material for certain types of metrology. Raman spectroscopy is a very useful technique that can provide non-invasive and spatially-resolved material information [31]. Through the analysis of inelastically scattered light, combined with confocal microscopy or surface enhancements, molecular signatures can be obtained. This information can be used to observe liposome nanoparticle uptake [32], the flow of nutrients in a cell [33], differentiate between cardiomyocyte phenotype [34] and discriminate the location of nucleic acids [35].

Raman imaging of cells on glass or a permeable polycarbonate substrate would produce an intrusive background signal that obscures signals originating from biomolecules, providing a source of error in the measurement. For this reason, Raman imaging of *in vitro* cell culture has been traditionally performed on thin pieces of magnesium fluoride. However, a magnesium fluoride ($MgF_2$) substrate does not have the necessary permeability needed to study the barrier properties of cultured epithelium. Substrate permeability is also necessary for proper cell phenotype [36, 37], as epithelial cells are known to polarize on permeable, but not impermeable substrates. Thus, the study of water transport across epithelial cells requires a nanomembrane made of $MgF_2$. The thinness of a $MgF_2$ nanomembrane will also mimic the dimensions of the basement membrane of barrier tissue (20-100 nm).

In this Aim, we hypothesize that it is possible to create a porous nanomembrane that minimizes oppressive Raman spectroscopy background signals and can be integrated into microsystems. To accomplish this objective, we will attempt to evaporate $MgF_2$ onto a standard nanomembrane made of silicon nitride. Subsequent removal of the silicon nitride using reactive ion etch will create a substitute $MgF_2$ nanomembrane, producing a silent Raman background for cell imaging and transport studies. The successful completion of this Aim will not only produce nanomembranes appropriate for Raman imaging, it will demonstrate a method to expand the nanomembrane platform to new materials

## Research Design

### 2.1 $MgF_2$ Nanomembrane Fabrication via Silicon Substitution

Creation of a $MgF_2$ nanomembrane is paramount to enabling measurements and water flux across epithelial monolayers. Starting from a commercially available nanoporous silicon nitride substrate (SiMPore inc.), $MgF_2$ will be thermally evaporated at a rate of 0.1-0.3 nm/sec, producing a film that is 50 nm thick. This thickness is enough to produce a cohesive film, but still preserve the nanoporous characteristic of the substrate, albeit with smaller pores, due to gradual infilling of nanopores as the evaporated film thickness increases. The materials will be strengthened with an annealing run in Argon at 600 C, and a free-standing membrane will then be produced by removing the starting silicon nitride substrate via reactive ion etching (RIE) using a mixture of $CHF_3$ (93.5%) and Oxygen (7.5%) with a 75 W plasma. Gold and platinum materials will also be fashioned into nanomembranes to test if the substitution technique can be generalized to other materials (Figure 3a).

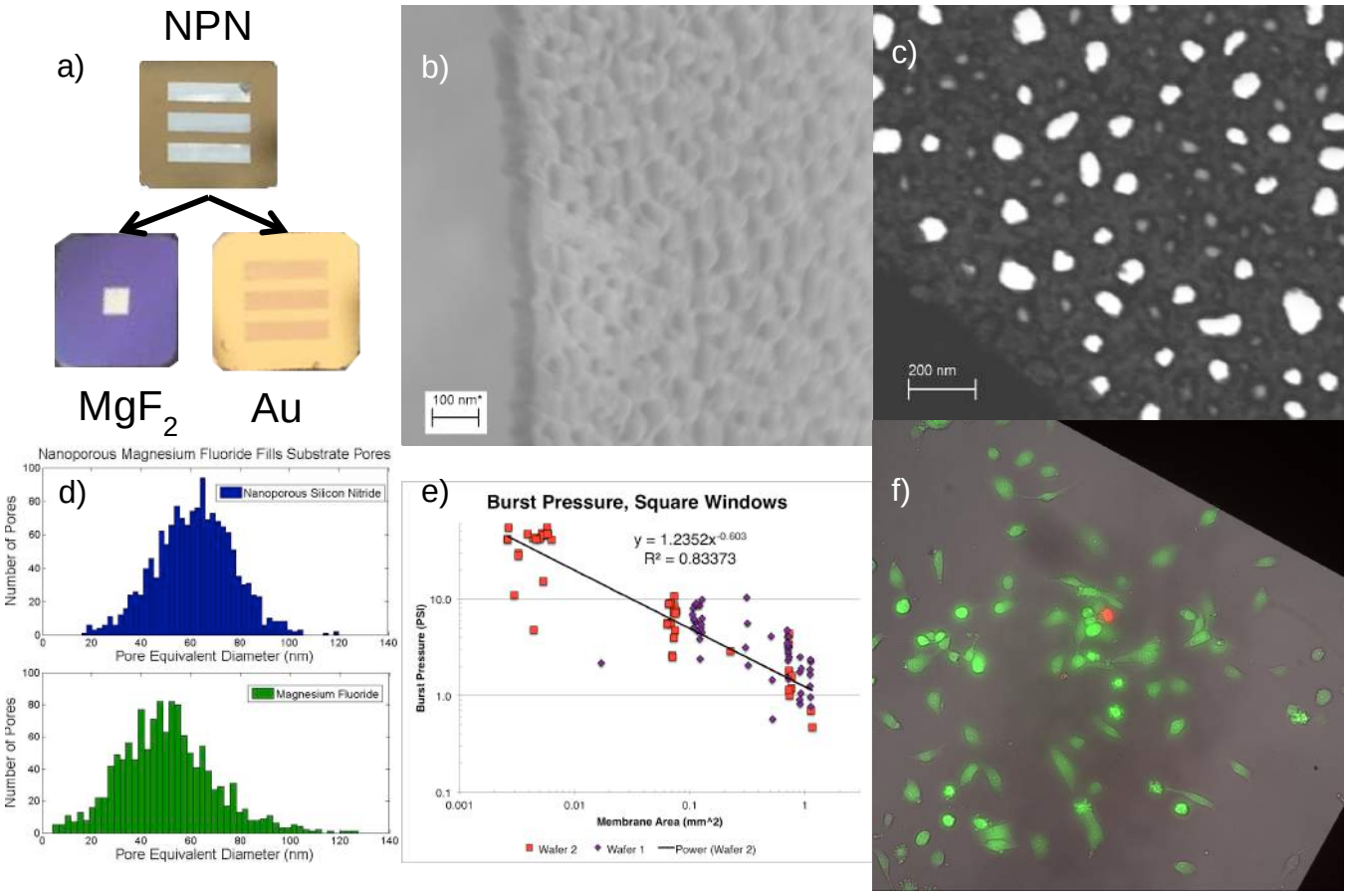


*Figure 2 – Nanoporous membrane fabrication by silicon substitution characterization. a) Nanoporous silicon nitride templating material can be changed into $MgF_2$ or Au nanomembranes. b) SEM crossection of fabricated $MgF_2$ nanomembrane (50 nm thick). c) STEM image displaying open nanopores in the $MgF_2$ nanomembrane. d) Pore histogram displaying that a $MgF_2$ nanomembrane will have reduced pore sizes compared to the template. e) Burst pressure study of $MgF_2$ square windows show that larger windows have smaller burst pressures. f) Live/Dead stain of P5 HUVECs grown on a 0.7x0.7 mm square $MgF_2$ nanomembrane show the material is cytocompatible.*

## 2.2 Mechanical and Material Characterization of Fabricated $MgF_2$ Nanomembranes

To determine practical sizes of the fabricated $MgF_2$ nanomembranes, we will compare the gas pressure necessary to rupture the nanomembrane with other silicon based nanomembranes. Pure silicon (pnc-Si) and silicon nitride nanomembranes of varying active areas (0.05 - 1 $mm^2$) will be subjected to differential pressures (0.1 - 20 PSI) using a pressure clamped system (Figure 3e). The burst pressures for these materials will then be compared to $MgF_2$ nanomembranes of the same window size. Given the brittle structure of the films, it is expected that the burst pressures will be comparable to the weaker pnc-Si nanomembranes than the stronger silicon nitride nanomembranes.

The material composition of the free-standing film will be verified using Energy Dispersive Spectometry (EDS) and X-ray Photoelectron Spectroscopy (XPS), providing evidence that the underlying silicon nitride template had been successfully removed (Appendix II). The physical structure of the membrane will be validated using Scanning Electron Microscopy (SEM) and Scanning Transmission Electron Microscopy (STEM), using the templating material as a control, counting pore distributions and shapes to establish that the fabricated membranes are similar to the templating material (Figure 3b, 3c, 3d).

$MgF_2$ nanomembranes must be biocompatible for use in cellular Raman imaging and should support the formation of tight monolayers for studies of barrier function. To evaluate compatibility with tissue barriers, we will culture vascular endothelial (HUVEC) cells on silicon nanomembranes, $MgF_2$ nanomembranes, and polycarbonate membranes in a transwell, static environment. Transepithelial Electrical Resistance (TEER) will be measured using a commercial TEER system (ENDOHM2, World Precision Instruments) as one measure of tissue barrier health (Figure 5a, 5b). As the barriers are cultured, the TEER will increase. Phase microscopy will be used to compare cell morphology across substrate types, and Live/Dead staining (L3224 kit, Invitrogen) will be used to confirm the material cytocompatibility (Figure 3f). At the end of this study, we will demonstrate cell viability on $MgF_2$ nanomembranes that is comparable to silicon-based nanomembranes.

### 2.3 Raman Background Characterization of Fabricated $MgF_2$ Nanomembranes

The Raman background of the fabricated nanomembranes will be verified via a Raman spectroscopic sweep across the deuterium and silicon peak regions compared against pnc-Si and $MgF_2$ coverglass materials. This will be accomplished by culturing retinal epithelial (ARPE-19) cells on the different substrates and gathering the spectrum using incident light of 660 nm at 100 mW, and an avalanche photodiode, carried out by the Webb laboratory at the University of Nottingham. It is expected that the large background peak from silicon will be eliminated, directly proportional to the amount of silicon present in the evaporated film (Figure 4). This, in turn, should increase the available laser power to interrogate cell samples, resulting in quicker measurements. At the end of this process, freestanding nanoporous $MgF_2$ nanomembranes will be fabricated that have significantly less background signal than state of the art silicon nanomembranes.

## Expected Outcomes

At the conclusion of this Aim, we will have created nanoporous $MgF_2$ nanomembranes that will facilitate Raman imaging of cells. Having characterized the material's Raman signature, porosity, cytocompatiblity, and mechanical structure, a new microsystem incorporating this substrate will allow spatially resolved measurement of water flux across a

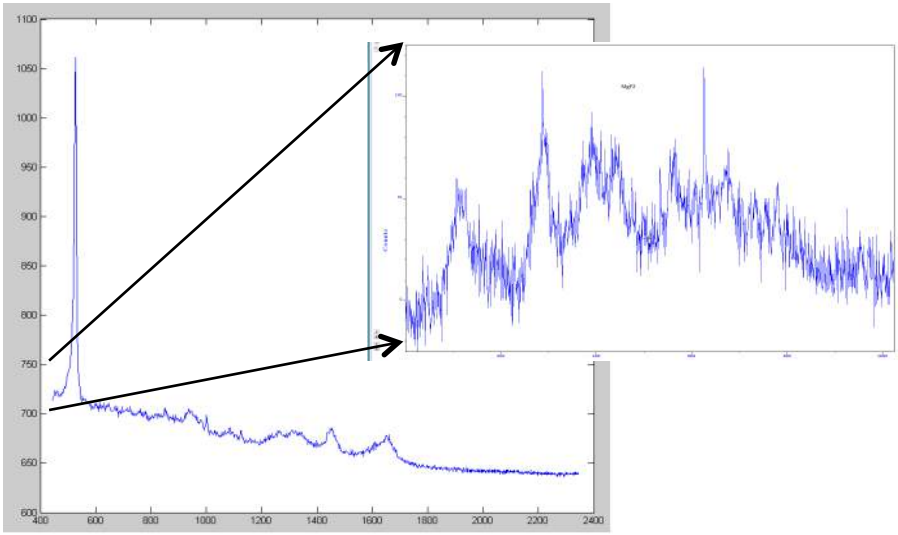


*Figure 4 – Raman signature of a pnc-Si nanomembrane and cell with a large silicon peak swamping out the rest of the signal. (inset) Raman signature of a $MgF_2$ nanomembrane and cell, lacking the silicon peak.*

cultured epithelial barrier using Raman spectroscopy in Aim 3. The fabricated membranes will have also demonstrated a method for extending the silicon nanomembrane platform to new materials.

### Potential Problems and Alternative Solutions

Fabrication and use of the $MgF_2$ nanomembranes has already been accomplished in practice, but if the material cannot support cell growth over a long period of time (weeks) without rupturing, it will be impossible to grow a confluent monolayer. It is possible to add additional processing steps that produce an additional silicon nitride superstructure to the magnesium fluoride, adding mechanical strength but remaining outside of the Raman observation window. The fabrication yield has traditionally been poor for $MgF_2$ (10-15%), but could be improved by optimizing the deposition rate, etch chemistry, and annealing step to maximize the strength of the formed nanomembranes.

## Specific Aim 3 Approach

### Hypothesis and Rationale

Epithelial transport is essential to cellular homeostasis, maintaining fluid and ion balance in the face of fluctuations from tissue function, both in response to normal physiology and to insult. Age related macular degeneration is a serious, prevalent condition that can eventually lead to blindness, thought to result in part from unregulated fluid transport by a damaged retinal pigment epithelial (RPE) layer [20, 21, 38]. Raman spectroscopy could be used to discretely measure water flux *in vitro,* but there are very few materials both cytocompatible and permeable that are compatible with this technique [31]. Therefore, we aim to quantify water transport for cultured RPE cells in a microsystem. A unique combination of material structure, composition, and manufacturing scalability make silicon-based nanomembranes promising for integration into microsystem metrology devices. Cellular physiology increasingly relies on multimodal characterization of behavior to unravel the complicated relationships between phenomena. We will enable discrete and bulk tracking of water fluxes through cultured RPE barriers by integrating Raman-compatibility via $MgF_2$ nanomembrane fabrication with miniaturized pump devices and flow sensors. This Aim will incorporate nanomembrane materials in LOC systems where they can serve as modular pumps, screens, and Raman silent permeable scaffolds. Success in this Aim will not only create a functional microsystem for the study of fluid transport across the retinal epithelium, it will demonstrate the broader theme of this thesis and nanomembranes represent a platform for the integration of multiple functions in microsystem design

We hypothesize that a microsystem incorporating $MgF_2$ nanomembranes (Aim 2) and silicon nitride nanomembranes can produce the necessary conditions to make multimodal quantifications of water transport. Both miniaturized pumping and sensing characteristics will be necessary to gather measurements in the confined space of a Raman microscope. Previous research has established that pnc-Si membranes exhibit low-loss, high-resolution molecular separations and give record permeabilities to both convecting and diffusing species [1]. Experiments have also demonstrated that silicon nanomembranes can function as electroosmotic pumps with efficiencies more than 20 times that of existing materials [4]. The silicon nanomembrane platform will be used here as scalable, modular pumps and sensors on a LOC device. At the successful completion of this Aim, we will have constructed a microsystem enabled by the nanomembrane platform that can directly assess epithelial water flux using noninvasive Raman spectroscopy, adaptable to other barrier tissue disease models.

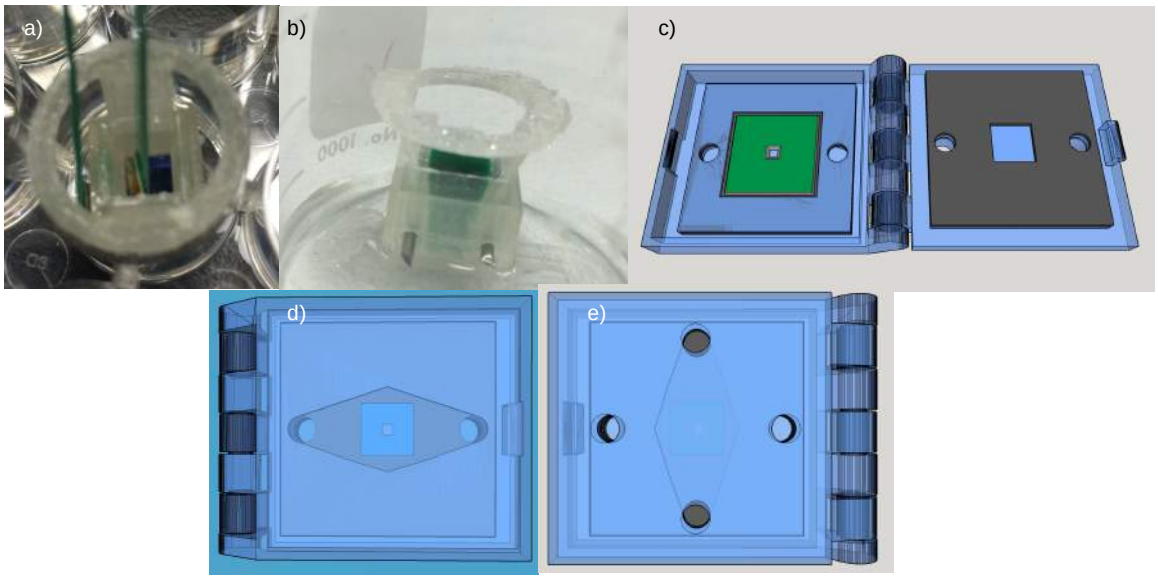


*Figure 5 – RPE Cell Culture Microsystem. a) Cells grown in a 24 well-plate using a 3d printed transwell format. b) Cell confluence will be established using TER measurements. c) Open device with one chip inserted. Blue areas are plastic, and gray areas are silicone. The chip is represented as a green square, 5.4 mm x 5.4 mm. The device is 4 mm thick, but the overall working distance is 800 µm to the nanomembrane layer from the bottom. d) Bottom view. e) Top view.*

## Research Design

### 3.1 Fabrication and Characterization of a Nanomembrane Flow Sensor and Pump

The direct relationship between water flow in a capillary and the generation of voltage is necessary to create effective miniaturized pumps. This relationship is quantified by the zeta potential of the material which is interacting with the water. Streaming potential measurements on different nanomembranes (NPN, Au, $MgF_2$) will be made by using a pressure-driven system (0.1-10 PSI) to drive 10 mM KCl (buffered to pH 7.2) through each nanomembrane and the generated voltage across the membrane will be recorded to derive the zeta potential. Knowing this information, we can then make predictions about the effective electroosmotic pumping of the different materials. Larger zeta potentials result in a stronger pumping effect. By applying a small differential voltage through Ag/AgCl electrodes (2 V), we can generate µL/min flows in a 0.1 mm sized microchannel (PET laminate carved with craft cutter) and check this performance of the material. This study will inform the design of pumps and sensors in the future for different microsystems, across different membrane sizes, salt concentrations, and pH concentrations from previously established relationships [4].

### 3.2 Integration of a Nanomembrane Pump, Raman Scaffold, and Flow Sensor into a Microsystem

While it is immediately desirable to fabricate different material regions on the same chip it can be costly to do so in a research space where channel length savings can only be a few mm. It is easier to produce chips of different material and separately integrate them into a platform with other elements specialized for measurements. Therefore, $MgF_2$ and NPN nanomembrane chips will then be placed in a resealable clamp, fabricated using a combination of 3d printed Objet VeroClear plastic and silicone gaskets that form the microfluidic channels, conduits, and electrode port insertions (Figure 5). This microsystem will be designed to fit within a small observation space (~25 mm diameter circle) on a Raman microscope, permitting measurements to be made on cells grown on chips that are inserted into the system.

### 3.3 Rapid Raman Measurement of Epithelial Water Flux with a Deuterium Tracer

Using the materials developed in sections 2.3, 3.1, and 3.2, we will grow RPE (ARPE-19) cells to confluence in a 24-well plate transwell configuration, evaluating confluence with TEER measurement as in Section 2.1. These $MgF_2$ chips will be inserted into a 2-channel microsystem containing a $MgF_2$ coverglass floor and roof, maintaining Raman compatible materials within the optical beam path (Figure 5). Using deuterated water as a tracer [39], we will inject water on the basolateral side of the cell layer and run a line-scan of the Raman beam across the cell boundaries and soma. This will provide time-resolved, spatially resolved measurements of epithelial water flux as the confluent layer pumps, where peaks of deuterated water (2400 $cm^{-1}$) are expected around the paracellular pathway. Principal component analysis will be used to separate out the water signatures from other material signatures in the system.

### 3.4 Measurement of Epithelial Water Flux with Integrated Nanomembrane Streaming Potential Measurements

Optical quantification using Raman spectroscopy of the fluid flow is useful as it provides discrete measurements of the water transport, however, this method has a narrow field of view of only a few cells. To characterize the bulk behavior of the fluid transport governed by the epithelial layer, we will use integrated nanomembrane streaming potential sensors (incorporated into the clamp) to measure flow rates within the system, adjusting the pumping rate of the ARPE-19 cells by osmotic challenge and pH concentration. Once this relationship is established, we will attempt to stall out the pumping of the cells by generating pressure with electroosmotic pump chips (incorporated into the clamp), and concurrently observe the results with Raman spectroscopy and phase microscopy. This study will have demonstrated the ability of a nanomembrane platform microsystem to control and sense the miniaturized environment of a LOC tissue model.

## Expected Outcomes

At the successful completion of this Aim, we will have characterized and fabricated silicon nanomembrane microsystem elements that permit direct, non-invasive, multimodal methods of characterizing water transport. Microsystems designed using the silicon nanomembrane platform can take advantage of the many different modes of operation of these nanomembranes to miniaturize and integrate into existing measurement setups. The microsystems have the potential to be produced at larger volumes to increase fidelity of these sensitive measurements further through repetition.

## Potential Problems and Alternative Solutions

While there are many ways to tackle the fabrication of tiny integrated microsystems other than the methods outlined here, the single largest point of failure in this Aim would be an unhealthy cell layer. To make a believable model of epithelial fluid transport, the measurement of cells within the system must not significantly change the cell layer. The combined effects of voltage application, fluid shear, deuterated water, osmotic challenge, pH adjustment, and laser power may provide a challenge to barrier integrity over time. Individually, each of the electrical, optical, and mechanical techniques have been used in other organ-on-a-chip models, but the confluence of all of them together may produce something unexpected. If these effects are

obvious, we may operate in a lower power regime, or separate measurements so that they are not concurrent, allowing some time for the cells to recover from a shock.

A drawback to resealable systems is that they are often more prone to leakage compared to permanently affixed systems. Using a 3d printed, resealable tissue clamp that has a wet interface may be problematic if the conductive media can make contact around the substrate chips through the gaskets. This would short out many of the desired nanomembrane behaviors. An alternative strategy would be to create individual, permanently bonded microsystems out of $MgF_2$ and culture cells within them, integrating individual pumps and sensors to each system.

## Summary/Timeline

Work in this proposal validates the use of silicon nanomembrane technology as a platform for improving microsystems, by introducing functional elements that impact the ability of microsystems to function. Used as individual elements *post-hoc* or designed for use *pre-hoc*, silicon nanomembrane technology will improve our ability to make clean, specific measurements, filter out garbage from samples, drive flows without mechanical pumping and sense similarly tiny fluid flows. These advantages will have made a significant impact on improving devices that will become a necessity in healthcare, as well as experimental devices to understand and illuminate the base physiology for tissue barrier diseases.

The successful completion of these aims should take no more than 2 years, given the present status on the development of the materials and integration efforts. The first year will be spent at the University of Nottingham, UK, approaching Aims 2 and 3, where an independent arrangement to work with a Raman microscope and 3d printing facility has been established. The remainder of the time will be used to establish DNA translocations and test models of wetting described in Aim 1.

# Appendix – Supporting Figures

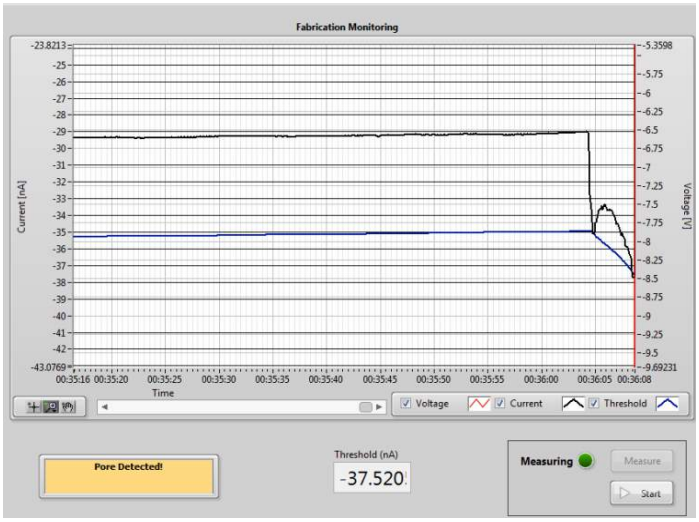


*Appendix I – Current profile of a successful nanopore drilling event through a tented nanomembrane structure, using a breakdown voltage of 15 V. As the nanopore is formed, the shunt current between source and drain dramatically increases, which is then controlled before enlarging the new pore substantially.*

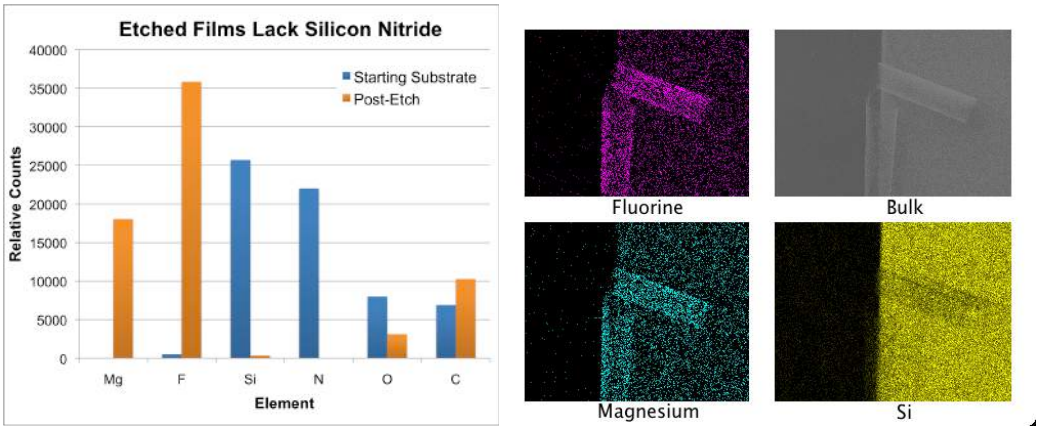


*Appendix II – Elemental Characteristics of Fabricated $MgF_2$ film. Left – XPS data of a sample templating membrane and fabricated $MgF_2$ nanomembrane (post-etch). Right – EDS scan of a broken, curled nanomembrane on the surface. The fabricated film in the free standing region (85% $MgF_2$) is lacking silicon.*

# Bibliography


1. Striemer, C.C., et al., *Charge- and size-based separation of macromolecules using ultrathin silicon membranes.* Nature, 2007. **445**(7129): p. 749-753.
2. Gaborski, T.R., et al., *High-Performance Separation of Nanoparticles with Ultrathin Porous Nanocrystalline Silicon Membranes.* ACS Nano, 2010. **4**(11): p. 6973-6981.
3. Chung, H.H., et al., *Highly permeable silicon membranes for shear free chemotaxis and rapid cell labeling.* Lab on a Chip, 2014. **14**(14): p. 2456-2468.
4. Snyder, J.L., et al., *High-performance, low-voltage electroosmotic pumps with molecularly thin silicon nanomembranes.* Proceedings of the National Academy of Sciences, 2013. **110**(46): p. 18425-18430.
5. Rae, A., et al., *State of the art Raman techniques for biological applications.* Methods, 2014. **68**(2): p. 338-347.
6. Fischbarg, J., *Fluid Transport Across Leaky Epithelia: Central Role of the Tight Junction and Supporting Role of Aquaporins*. Vol. 90. 2010. 1271-1290.
7. Dittrich, P.S. and A. Manz, *Lab-on-a-chip: microfluidics in drug discovery.* Nat Rev Drug Discov, 2006. **5**(3): p. 210-218.
8. Fair, R.B., *Digital microfluidics: is a true lab-on-a-chip possible?* Microfluidics and Nanofluidics, 2007. **3**(3): p. 245-281.
9. Chin, C.D., V. Linder, and S.K. Sia, *Commercialization of microfluidic point-of-care diagnostic devices.* Lab on a Chip, 2012. **12**(12): p. 2118-2134.
10. Mijatovic, D., J. Eijkel, and A. Van Den Berg, *Technologies for nanofluidic systems: top-down vs. bottom-up—a review.* Lab on a Chip, 2005. **5**(5): p. 492-500.
11. Nie, Z., et al., *Polymer Particles with Various Shapes and Morphologies Produced in Continuous Microfluidic Reactors.* Journal of the American Chemical Society, 2005. **127**(22): p. 8058-8063.
12. Gijs, M.M., *Magnetic bead handling on-chip: new opportunities for analytical applications.* Microfluidics and Nanofluidics, 2004. **1**(1): p. 22-40.
13. Booth, R. and H. Kim, *Characterization of a microfluidic in vitro model of the blood-brain barrier ([small mu ]BBB).* Lab on a Chip, 2012. **12**(10): p. 1784-1792.
14. Ni, J., B. Li, and J. Yang, *A pneumatic PDMS micropump with in-plane check valves for disposable microfluidic systems.* Microelectronic Engineering, 2012. **99**(0): p. 28-32.
15. Ogden, S., et al., *Review on miniaturized paraffin phase change actuators, valves, and pumps.* Microfluidics and Nanofluidics, 2014. **17**(1): p. 53-71.
16. Jahanshahi, A., F. Axisa, and J. Vanfleteren, *Fabrication of a biocompatible flexible electroosmosis micropump.* Microfluidics and Nanofluidics, 2012. **12**(5): p. 771-777.
17. Kumar, R., et al., *Nongassing Long-Lasting Electro-osmotic Pump with Polyaniline-wrapped Aminated Graphene Electrodes.* ACS Applied Materials & Interfaces, 2014. **7**(1): p. 593-601.
18. Briggs, K., H. Kwok, and V. Tabard-Cossa, *Automated Fabrication of 2-nm Solid-State Nanopores for Nucleic Acid Analysis.* Small, 2014. **10**(10): p. 2077-2086.
19. Schneider, G.F., et al., *Tailoring the hydrophobicity of graphene for its use as nanopores for DNA translocation.* Nat Commun, 2013. **4**.
20. de Jong, P.T.V.M., *Age-Related Macular Degeneration.* New England Journal of Medicine, 2006. **355**(14): p. 1474-1485.

21. Holz, F.G., S. Schmitz-Valckenberg, and M. Fleckenstein, *Recent developments in the treatment of age-related macular degeneration.* The Journal of clinical investigation, 2014. **124**(4): p. 1430-1438.
22. Jain, T., et al., *Integration of Solid-State Nanopores in Microfluidic Networks via Transfer Printing of Suspended Membranes.* Analytical Chemistry, 2013. **85**(8): p. 3871-3878.
23. Bootman, J.L., *The Convergence of New Technology With the Delivery of Health Care Services.* American journal of pharmaceutical education, 2013. **77**(1).
24. Schadt, E.E., S. Turner, and A. Kasarskis, *A window into third-generation sequencing.* Human Molecular Genetics, 2010. **19**(R2): p. R227-R240.
25. Niedringhaus, T.P., et al., *Landscape of Next-Generation Sequencing Technologies.* Analytical Chemistry, 2011. **83**(12): p. 4327-4341.
26. Dekker, C., *Solid-state nanopores.* Nat Nano, 2007. **2**(4): p. 209-215.
27. Schneider, G.F. and C. Dekker, *DNA sequencing with nanopores.* Nature biotechnology, 2012. **30**(4): p. 326-328.
28. Eisenstein, M., *Oxford Nanopore announcement sets sequencing sector abuzz.* Nature biotechnology, 2012. **30**(4): p. 295-296.
29. Branton, D., et al., *The potential and challenges of nanopore sequencing.* Nat Biotech, 2008. **26**(10): p. 1146-1153.
30. Berthold, A., et al., *Glass-to-glass anodic bonding with standard IC technology thin films as intermediate layers.* Sensors and Actuators A: Physical, 2000. **82**(1–3): p. 224-228.
31. Kann, B., et al., *Raman microscopy for cellular investigations — From single cell imaging to drug carrier uptake visualization.* Advanced Drug Delivery Reviews, (0).
32. Matthäus, C., et al., *New Ways of Imaging Uptake and Intracellular Fate of Liposomal Drug Carrier Systems inside Individual Cells, Based on Raman Microscopy.* Molecular Pharmaceutics, 2008. **5**(2): p. 287-293.
33. Yamakoshi, H., et al., *Imaging of EdU, an Alkyne-Tagged Cell Proliferation Probe, by Raman Microscopy.* Journal of the American Chemical Society, 2011. **133**(16): p. 6102-6105.
34. Ghita, A., et al., *Applications of Raman micro-spectroscopy to stem cell technology: label-free molecular discrimination and monitoring cell differentiation.* EPJ Techniques and Instrumentation, 2015. **2**(1): p. 1-14.
35. Salic, A. and T.J. Mitchison, *A chemical method for fast and sensitive detection of DNA synthesis in vivo.* Proceedings of the National Academy of Sciences, 2008. **105**(7): p. 2415-2420.
36. Pfeffer, B.A. and N.J. Philp, *Cell culture of retinal pigment epithelium: Special Issue.* Experimental Eye Research, 2014. **126**(0): p. 1-4.
37. Dunn, K.C., et al., *ARPE-19, A Human Retinal Pigment Epithelial Cell Line with Differentiated Properties.* Experimental Eye Research, 1996. **62**(2): p. 155-170.
38. Ding, X., M. Patel, and C.-C. Chan, *Molecular pathology of age-related macular degeneration.* Progress in Retinal and Eye Research, 2009. **28**(1): p. 1-18.
39. Iaroslavskaia, A., et al., *[Water exchange in human crystalline lens studied by combined dispersion confocal microspectroscopy].* Biofizika, 1997. **43**(1): p. 125-130.